Original Article

3D time-of-flight magnetic resonance angiography of lenticulostriate artery imaging at 5.0 Tesla: a hierarchic analysis method and clinical applications

Hao Mei[1#], Jinfeng Lv[1#], Dan Xu[1], Lei Gao[1], Wenbo Sun[1], Xiaoli Zhong[1], Chenhong Fan[1], Ran Tao[2], Xiaopeng Song[3,4], Feng Xiao[1*], Haibo Xu[1*]

[1]Department of Radiology, Zhongnan Hospital of Wuhan University, Wuhan, China; [2]Department of Radiology, Union Hospital, Tongji Medical College, Huazhong University of Science and Technology, Wuhan, China; [3]MR Collaboration, Central Research Institute, United Imaging Healthcare, Shanghai, China; [4]Wuhan Zhongke Industrial Research Institute of Medical Science, Wuhan, China

Contributions: (I) Conception and design: H Xu, F Xiao, H Mei, J Lv; (II) Administrative support: H Xu, W Sun, X Song; (III) Provision of study materials or patients: H Mei, J Lv; (IV) Collection and assembly of data: W Sun, X Zhong, C Fan, R Tao; (V) Data analysis and interpretation: H Mei, J Lv, L Gao, F Xiao; (VI) Manuscript writing: All authors; (VII) Final approval of manuscript: All authors.

[#]These authors contributed equally to this work as co-first authors.

[*]These authors contributed equally to this work.

Correspondence to: Haibo Xu, PhD; Feng Xiao, PhD. Department of Radiology, Zhongnan Hospital of Wuhan University, 169 East Lake Road, Wuhan 430000, China. Email: xuhaibo@whu.edu.cn; xiao.feng@whu.edu.cn.

Background: Lenticulostriate artery (LSA) arteriosclerosis is a key pathological basis for cerebrovascular diseases including stroke and cerebral small vessel disease. However, the comprehensive visualization and the meticulous quantitative analysis of the entire spectrum of LSA branches remain an ongoing clinical challenge. This study aimed to explore the efficacy of LSA branch detection using ultra-high field clinical 5.0 Tesla (T) magnetic resonance imaging (MRI) with 3D time-of-flight (TOF) magnetic resonance angiography (MRA) and to introduce a hierarchic categorization method for better LSA branching pattern analysis.

Methods: A total of 12 participants were included and scanned using 5.0T and 3.0T TOF-MRA. First, an LSA hierarchic analysis method that categorized the LSA into three levels was proposed. Morphological parameters and signal-to-noise ratio/contrast-to-noise ratio (SNR/CNR) were calculated separately at each level. Then, the LSA imaging quality was compared between 5.0T and 3.0T TOF-MRA, utilizing the hierarchic analysis method. Next, the resolution setting in 5.0T TOF-MRA was optimized for better LSA imaging. Finally, the patient with left cerebral infarction underwent a 4-month follow-up examination using 5.0T TOF-MRA to validate the clinical utility of the 5.0T TOF-MRA and the proposed hierarchic analysis method.

Results: The LSA imaging quality on 5.0T is significantly better than that of 3.0T in different levels of the LSA branches both in the numbers and lengths ($P<0.05$). Critically, LSA tertiary branches which were commonly delineated in the 5.0T TOF-MRA images were barely visible in the 3.0T images; furthermore, at the origin of LSA branches, 5.0T TOF-MRA showed notably superior visualization in comparison to the 3.0T ($P<0.001$). The clinical application studies showed the advantageous prospects of the proposed quantitative analysis method for LSA-related research at 5.0T.

Conclusions: The visibility in the branching of LSA with 5.0T TOF-MRA is superior to that of 3.0T, especially at the origination from the middle cerebral artery (MCA) and the periphery of its branches. With the implementation of the proposed hierarchic analysis method for LSA, 5.0T TOF-MRA could be

a valuable instrument for identifying subtle changes in LSA associated with various cerebrovascular-related diseases.

Keywords: Lenticulostriate vascular diseases; magnetic resonance angiography (MRA); magnetic resonance imaging (MRI); 5.0 Tesla (5.0T)

Submitted Jul 30, 2024. Accepted for publication Jan 13, 2025. Published online Feb 26, 2025.
doi: 10.21037/qims-24-1554
View this article at: https://dx.doi.org/10.21037/qims-24-1554

Introduction

Lenticulostriate arteries (LSAs) are the perforating branches of the middle cerebral artery (MCA) and supply blood to the basal ganglia and the internal capsule (1,2). Ischemic and hemorrhagic cerebral strokes often occur in the territories of these perforating arteries, which account for 20% of all strokes and 35–44% of intracerebral hemorrhages (3). Therefore, visualizing the entire spectrum of LSA branches can provide valuable insights into the pathophysiological mechanism of cerebrovascular diseases, which are important for diagnosis and prognosis.

Time-of-flight (TOF) magnetic resonance angiography (MRA), a non-invasive vascular imaging modality, stands as a crucial tool for intracranial artery visualization (4,5). TOF-MRA has been employed on conventional 3.0 Tesla (T) and 1.5T magnetic resonance imaging (MRI) systems to visualize LSA branches (6-8). However, the clinical potential of TOF is challenged by the low detection rate of LSA branches. For instance, Gotoh *et al.* reported that the average length of LSA was 59.5 mm, which is significantly less than empirical data show (9). Some studies have suggested that 7.0T MRI can improve the visualization of LSA (10-16). However, due to safety issues such as high specific absorption rate (SAR), and technical issues such as B1 field inhomogeneity, as well as the limited availability, achieving high-quality images outside the brain is a challenge for 7.0T MRI, which limits its broader clinical application. At present, ultra-high field clinical 5.0T MRI provides a balance between image quality and safety, and some studies have suggested that 5.0T MRI can visualize distal brain arteries and small vascular branches, and the image quality is comparable to 7.0T (17-19). Therefore, this study focused on the visualization of entire spectrum of LSA by using ultra-high field clinical 5.0T MRI.

In addition, it is believed that the point of occlusion of an LSA is related to the size and shape of the arteries where the infarction is located (7,20). A hierarchic categorization of the LSA branches based on their morphology is required for accurate localization and description of the infarctions. Some investigations have been undertaken in this domain. For instance, Kang *et al.* employed the TOF sequence at 7.0T ultra-high field MRI to analyze the morphology and number of LSA stem and branch, but did not calculate the length of stem and branch of LSA (10,15). Conversely, Ma *et al.* utilized black-blood method to calculate the number and length of LSA at 3.0T and 7.0T, respectively, but did not describe the different branches or topological hierarchy of LSA in detail (12). Additionally, in practical work, the simple classification of LSA into larger and smaller stems cannot accurately reflect the MRA image quality at different field strengths and the vascular changes of the distal segment. Hence, we proposed a hierarchic analysis method which divides the LSA into three different categories based on their morphology for in-depth analysis of LSA branching patterns.

In this investigation, we employed ultra-high field clinical 5.0T MR with the LSA hierarchic analysis method to systematically explore LSA and their branches. This approach is anticipated to offer researchers a valuable tool for discerning and delineating subtle alterations in the branching pattern of LSA, thereby enabling the implementation of sophisticated and personalized interventions.

Methods

Study population

The study was conducted in accordance with the Declaration of Helsinki (as revised in 2013). The study was approved by the Medical Ethics Committee of Zhongnan Hospital of Wuhan University (No. 2021110) and all participants provided written informed consent. A total of 12 healthy participants were enrolled (5 males and 7 females, mean age: 26.25 years, age range: 21–35 years, standard deviation: 4.38 years) from February to July 2022.

Table 1 MR scanning parameters used in this study

Parameters	5.0T TOF-MRA			3.0T TOF-MRA
	0.5 mm	0.4 mm	0.3 mm	
Field of view (mm^2)	224×180	224×180	224×180	224×180
Acquisition voxel (mm^3)	0.5×0.5×0.5	0.4×0.4×0.4	0.3×0.3×0.3	0.5×0.5×0.5
Recon. voxel (mm^3)	0.25×0.25×0.25	0.2×0.2×0.2	0.15×0.15×0.15	0.25×0.25×0.25
TR/TE (ms)	20.0/4.1	20.6/4.8	21.1/4.8	19.5/5.2
Slab	3	3	3	3
Slice per slab	60	60	60	60
Gap	–25%	–25%	–25%	–25%
Slice interpolation	2	2	2	2
Number of slices	300	300	300	300
Slice oversampling (%)	20	20	20	20
Flip angle (°)	15	15	15	17
Band width (Hz/pixel)	250	250	250	250
Average	1	1	1	1
CS factor (uCS)	3.5	3.5	3.5	3.5
Tone	Medium	Medium	Medium	Medium
Scan duration (min)	7:02	9:35	12:18	6:51

MR, magnetic resonance; TOF-MRA, time-of-flight magnetic resonance angiography; Recon., reconstruction; TR, repetition time; TE, echo time; CS, compressed sensing; uCS, united imaging compressed sense.

All 12 participants underwent both 5.0T and 3.0T TOF-MRA. None the participants had a history of smoking, hypertension, diabetes mellitus, or brain infarction.

MRI protocol

We conducted our study using two scanners: a prototype whole-body 5.0T MR scanner (uMR Jupiter, United Imaging Healthcare, Shanghai, China) with 48 channels and a commercial 3.0T MR scanner (uMR 790, United Imaging Healthcare) with 32 channels, both equipped with a commercial 24-element head coil. Three slabs, positioned axially, parallel to the plane of the anterior commissure-posterior commissure (AC-PC) line, were acquired using the multiple overlapping thin slab acquisition (MOTSA) technique. Each slab consisted of sixty 0.5-mm-thick partitions (including 15 overlapping slices (25% per slab). Each participant was first scanned with 5.0T TOF-MRA and then 3.0T TOF-MRA on the same day. The interval between the two scans was restricted within 5 hours. Detailed imaging parameters for the 5.0T and 3.0T MRA are shown in *Table 1*. The repetition time (TR) and echo time (TE) could not be matched because of the limitations of SAR with the 5.0T MR system. To obtain the optimal LSA imaging quality for 5.0T TOF-MRA, different resolution settings (0.3, 0.4, and 0.5 mm) in 5.0T TOF-MRA were tested and compared.

Image analysis and evaluation method

In this study, we proposed a hierarchical quantitative analysis method based on TOF-MRA for detailed analysis of LSA branching patterns, which could be further used in LSA imaging quality assessment and LSA-related disease analysis. In this hierarchic method, LSA were divided into the stems [originating directly from the middle cerebral artery (MCA)] and three different levels of branches (originating from the superior, stems, or branches): primary, secondary, and tertiary branches. Then, the LSA stem/branches at different levels were tracked, classified, and quantified using the "Project" and "Filament" modules of Avizo's filament tools (Avizo, version 2019.1 Thermo Fisher Scientific, Waltham, MA, USA). The details of the LSA hierarchic analysis method (contained the TOF-MRA

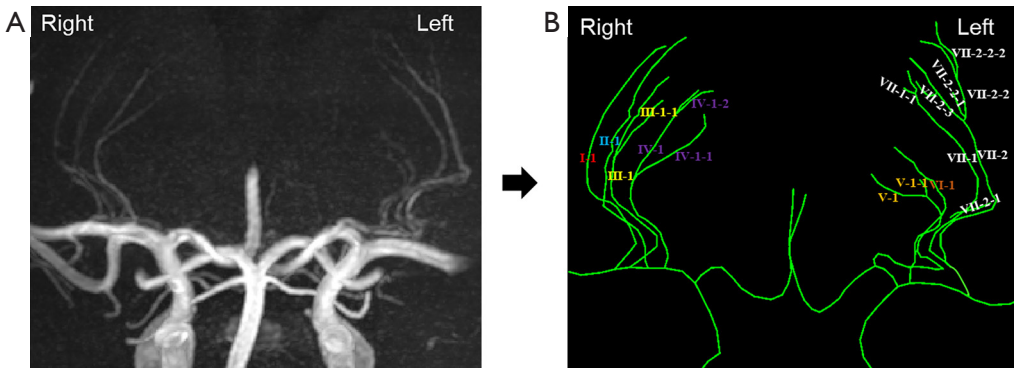

Figure 1 An example of LSA tracking and hierarchic scheme. (A) 5.0T TOF-MRA (maximum intensity projection, slab thickness =20 mm). (B) The tracking and division results for the LSA. The naming rule for the tracked LSA branches is stem-primary-secondary-tertiary. For example, VII-2-2-2 represents the detailed origin and course of this LSA branch. Counting from left to right, this vessel originates from the VII branch on middle cerebral artery (stem) and goes to this stem's second branch (primary); then it goes to this primary branch's second branch (secondary) and finally to the second branch of this secondary branch (tertiary), and so on. LSA, lenticulostriate artery; TOF-MRA, time-of-flight magnetic resonance angiography.

preprocess) are described below.

LSA image preprocessing

A commercial workstation (uMR workstation, version V10-3T, United Imaging) was used for the region of interest (ROI) crop before LSA analysis. All the redundant tissues in the image (e.g., scalp, skull, etc.) were removed; only the lenticulostriate area containing the LSA inside the skull was retained for subsequent analysis.

LSA tracking and display

The "Project" and "Filament" modules in a commercial software Avizo (Avizo, version 2019.1 Thermo Fisher Scientific) were used to track and display the LSA in three-dimensions.

Coarse segmentation: thresholding

The TOF images were binarized by adjusting an appropriate threshold (Project module of Avizo) to obtain a coarse segmentation of LSA. In general, the better the distant LSA were displayed, the more noise around the LSA was tagged. Therefore, the threshold setting should trade off LSA displaying quality against surrounding noise emerging.

Vessel skeleton extraction

The three-dimensional (3D) vascular skeleton of LSA was extracted using the "Auto Skeleton" function of AVIZO software, based on the LSA coarse segmentation result obtained in the previous step.

Manual fine-tuning and branch classification

After obtaining the 3D skeleton of the LSA, we manually checked and corrected (Filament module of AVIZO) two possible problems with the LSA vascular skeleton:

(I) Incorrect connections, which were caused by the complicated blood vessel structure and/or noise interference, were refined by disconnecting these connections and then removing isolated nodes.

(II) Lost distal LSA, which were caused by its low contrast and thin lumen, were revised through manually adding the distal vessels.

LSA hierarchic scheme

Following the identification of the LSA skeleton, different levels of LSA were identified and classified, as depicted in *Figure 1*. In detail, they were divided into different levels of stems and branches: stems were defined as the LSA that originated directly from the MCA, and branches were defined as daughter vessels originating from the parent LSA stems plus stems without any branches. Further, LSA branches were divided into three levels according to their originating sites: (I) primary branches are branches that originate directly from the stems plus stems without any branches; (II) secondary branches are branches that originate from the primary branches; and (III) tertiary branches are branches that originate from the secondary branches (*Figure 1*).

Hierarchic morphological parameters evaluation

On the basis of the proposed LSA hierarchic scheme, three hierarchic morphological parameters for the LSA were

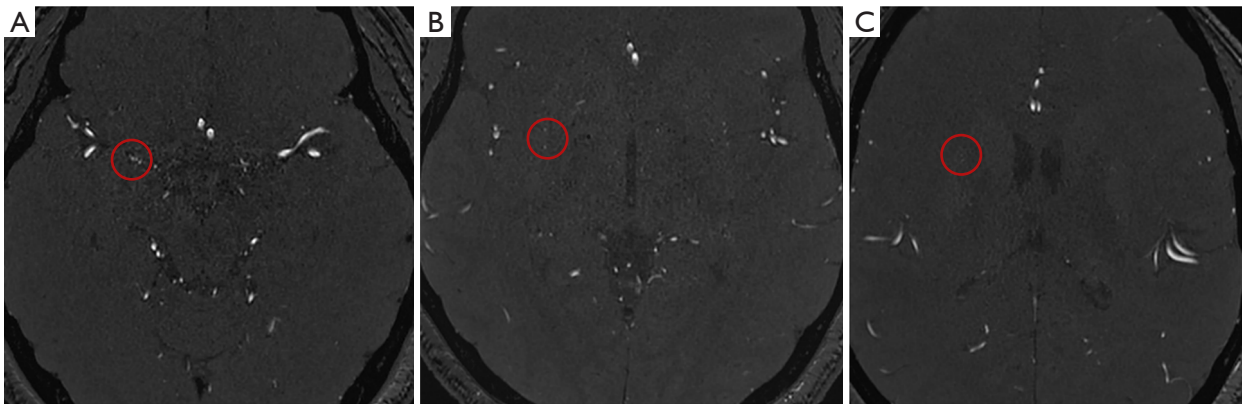

Figure 2 An example of the three slices of lenticulostriate arteries used in the traditional evaluation method based on SNR and CNR. From left to right, the subfigures correspond to the representative slices of stem/primary branches (A), secondary branches (B), and tertiary branches (C) used to measure the SNR and CNR. Red round frame: the specified place for the measurement. SNR, signal-to-noise ratio; CNR, contrast-to-noise ratio.

extracted: the number, length, and radius of LSA branches at different levels, which can be used to quantitatively evaluate the LSA for the participants.

(I) Branch number: total number of blood vessel branches at the current level.
(II) Branch length: total length of blood vessel branches at the current level.
(III) Branch radius: average radius of blood vessel branches at the current level.

In this study, two observers (H.M. and J.L.) assessed and measured the hierarchic morphological parameters of the LSA for the 12 participants, blinded to each other, and the intraclass correlation coefficient (ICC) was used to measure and evaluate the inter-observer reliability and test-retest reliability of these measurements.

Hierarchic signal-to-noise ratio (SNR) and contrast-to-noise ratio (CNR) evaluation

As shown in *Figure 2*, three ROI of LSA were separately delineated at the corresponding slice of the stem/primary branches, the secondary branches, and the tertiary branches of LSA for hierarchic evaluation. RadiAnt DICOM Viewer version 3.4.2 (Medixant, Poznan, Poland) was used in the procedure of ROI delineation and evaluation. To ensure the consistency of this procedure, all ROIs were delineated by the same author (R.T. with more than 10 years of experience in neuroimaging). In this study, the SNR was determined as the mean signal intensity of each ROI of different levels of LSA branches divided by the SD of the signal intensity in the noise background.

$$SNR = \frac{Mean\ of\ SI_{(LSA)}}{SD\ of\ SI_{(brain)}} \quad [1]$$

where SI denotes the signal intensity and SD represents the standard deviation. The definition of CNR was determined as:

$$CNR = \frac{Mean\ of\ SI_{(LSA)} - Mean\ of\ SI_{(brain)}}{SD\ of\ SI_{(brain)}} \quad [2]$$

In general, the ROI was placed on the brightest branch of the corresponding LSA branch artery. As the tertiary branches of some volunteers were too small to be accurately identified, the signal intensity was not measured.

5.0T vs. 3.0T TOF-MRA

To assess how magnetic field strength influences LSA imaging quality in TOF-MRA, we made a comparison between 5.0T and 3.0T based on the proposed hierarchic scheme. First, the branches of LSA were tracked and divided into different levels. Then, the morphological parameters and SNR/CNR of each branch were extracted, respectively. Finally, based on these metrics, the imaging quality of LSA under 5.0T and 3.0T MRI was compared.

5.0T TOF-MRA resolution parameter optimization

Higher magnetic field can result in higher imaging SNR. To fully explore the advantage of 5.0T ultra-high magnetic

Table 2 Detailed results for the repeated ANOVA analysis of the SNR and CNR between different resolutions settings

Feature	ANOVA results		Comparison (mm)	Estimate	P value
	F	P value			
Stem/primary SNR	22.31	<0.001***	0.3 *vs.* 0.4	−9.34	0.001**
			0.3 *vs.* 0.5	−16.27	<0.001***
			0.4 *vs.* 0.5	−6.92	0.022*
Stem/primary CNR	11.71	<0.001***	0.3 *vs.* 0.4	−6.7	0.007**
			0.3 *vs.* 0.5	−9.77	<0.001***
			0.4 *vs.* 0.5	−3.07	0.436
Secondary SNR	8.62	<0.001***	0.3 *vs.* 0.4	−4.55	0.134
			0.3 *vs.* 0.5	−9.11	<0.001***
			0.4 *vs.* 0.5	−4.56	0.133
Secondary CNR	3.59	0.037*	0.3 *vs.* 0.4	−2.77	0.226
			0.3 *vs.* 0.5	−3.96	0.038*
			0.4 *vs.* 0.5	−1.19	1.00
Tertiary SNR	15.17	<0.001***	0.3 *vs.* 0.4	−5.63	<0.001***
			0.3 *vs.* 0.5	−6.97	<0.001***
			0.4 *vs.* 0.5	−1.33	0.932
Tertiary CNR	3.8	0.031*	0.3 *vs.* 0.4	−2.22	0.016*
			0.3 *vs.* 0.5	−0.97	0.622
			0.4 *vs.* 0.5	1.25	0.312

*, P<0.05; **, P<0.01; ***, P<0.001. ANOVA, analysis of variance; SNR, signal-to-noise ratio; CNR, contrast-to-noise ratio.

field and obtain better LSA imaging quality, the influence of the parameter setting of resolution was explored. Three different resolutions settings (0.3, 0.4, and 0.5 mm) were used in this comparison to obtain the best LSA imaging quality in 5.0T TOF-MRA. Similar with the previous section, both morphological parameters and CNR/SNR were used to compare the imaging quality of the LSA with different resolution settings in the 5.0T TOF-MRA, and then used to evaluate and compare the imaging effect of LSA with different resolution settings, so as to obtain the optimal resolution setting of 5.0T TOF-MRA for LSA imaging.

Clinical application: a follow-up case study of a patient with left cerebral infarction

To illustrate and validate our approach's clinical utility, we conducted a follow-up case study on a cerebral infarction patient. His cerebral vessel images were captured using 5.0T TOF-MRA, and his LSA were analyzed and evaluated over a 4-month period using our proposed method (1, 73, and 126 days after the symptom onset respectively).

Statistical analysis

All the metrics (including SNR, CNR, and the LSA morphological parameters) extracted from TOF-MRA for the participants were compared between two groups using a paired sample *t*-test (5.0T *vs.* 3.0T, 0.3 *vs.* 0.4 mm, 0.4 *vs.* 0.5 mm, 0.3 *vs.* 0.5 mm), and among three groups (0.3 *vs.* 0.4 *vs.* 0.5 mm) using one-way repeated measures analysis of variance (ANOVA), and we included multiple comparisons with Bonferroni correction, see *Table 2*. The ICC analysis was used to measure and evaluate the inter-observer and test-retest reliability of observations for the LSA morphological parameters (stem/branches number, length, and radius). All statistical analyses in

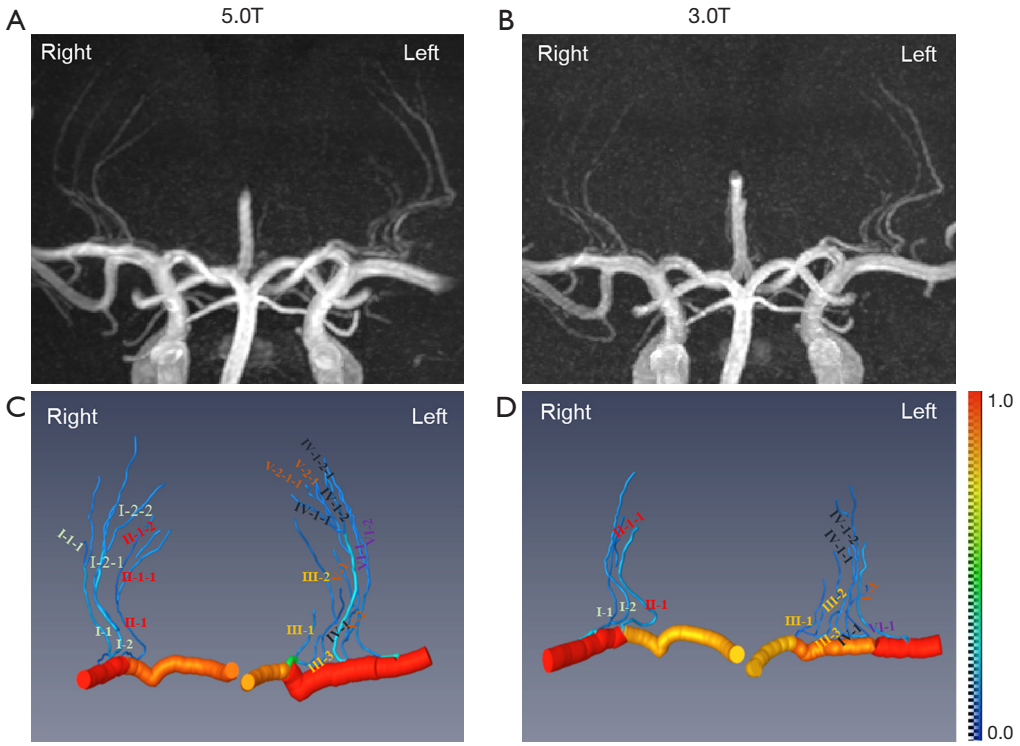

Figure 3 The maximum intensity projections of the 5.0T and 3.0T TOF-MRA, with a slab thickness of 20 mm, for a single volunteer (a 26-year-old female) were analyzed, and the stems and branches of the lenticulostriate arteries were extracted using pattern analysis. (A,C) The 5.0T TOF-MRA shows four stems, four primary, and three secondary branches in the right hemisphere, and three stems, four primary, five secondary, and two tertiary branches in the left hemisphere. (B,D) The 3.0T TOF-MRA shows four stems, four primary, and one secondary branches in the right hemisphere, and three stems and four primary branches in the left hemisphere. No tertiary and less secondary branching can be found at 3.0T. TOF-MRA, time-of-flight magnetic resonance angiography.

this study were conducted using the R software, version 4.3.0 (R Foundation for Statistical Computing, Vienna, Austria), with a two-sided P<0.05 considered statistically significant.

Results

As illustrated in *Figures 1*,*3*, we first categorized LSA branches into three distinct levels for all participants. We then extracted their corresponding LSA hierarchic morphological parameters and SNR/CNR metrics for further analysis. The ICC of LSA hierarchic morphological parameters shown in *Table 3* demonstrates that the proposed method and evaluation metrics were reliable and reproductive (except tertiary Num which is only moderately consistent; all other parameters are good consistent or excellent consistent).

5.0T TOF-MRA vs. 3.0T TOF-MRA

LSA branching patterns are more visibly defined in 5.0T TOF-MRA compared to 3.0T TOF-MRA. In the 5.0T TOF-MRA images of 12 participants (24 hemispheres), a total of 78 stems and 221 branches in total were tracked, comprising 114 primary branches (51.76%), 86 secondary branches (39.09%), and 20 tertiary branches (9.09%). In contrast, in 3.0T TOF-MRA, 58 stems and 133 branches could be tracked in total, which included 83 primary branches (62.41%) and 50 secondary branches (37.59%). Remarkably, no tertiary branches could be tracked from the 3.0T TOF-MRA images. 5.0T TOF-MRA was capable of displaying ultra-tiny branches with slow blood flow, such as certain distal tertiary branches (*Figure 4*, green rectangle), and even primary and secondary branches undetectable by 3.0T TOF-MRA (*Figure 4*, red dashed box). Additionally, 5.0T TOF-MRA can also display more details at the origin

Table 3 ICC analysis of LSA stems/branches measurement results

Parameters	ICC (95% CI)	
	3.0T TOF-MRA	5.0T TOF-MRA
Stem Num.	0.964 (0.880–0.990)	0.959 (0.864–0.988)
Stem Radius	0.963 (0.879–0.989)	0.922 (0.763–0.976)
Total Num.	0.985 (0.951–0.996)	0.951 (0.840–0.986)
Total Len.	0.946 (0.797–0.985)	0.943 (0.821–0.983)
Primary Num.	0.918 (0.748–0.975)	0.784 (0.410–0.933)
Primary Len.	0.967 (0.890–0.990)	0.855 (0.570–0.956)
Primary Radius	0.920 (0.747–0.976)	0.889 (0.660–0.967)
Secondary Num.	0.927 (0.765–0.978)	0.941 (0.816–0.982)
Secondary Len.	0.808 (0.430–0.942)	0.954 (0.854–0.986)
Secondary Radius	0.959 (0.869–0.988)	0.811 (0.485–0.941)
Tertiary Num.	–	0.664 (0.194–0.889)
Tertiary Len.	–	0.888 (0.662–0.966)

ICC <0.5: poor consistency; 0.5≤ ICC <0.75: moderate consistency; 0.75≤ ICC <0.9: good consistency; ICC ≥0.9: excellent consistency. ICC, intra-class correlation coefficient; LSA, lenticulostriate artery; TOF-MRA, time-of-flight magnetic resonance angiography; Num., number; Len., length; CI, confidence interval.

of LSA (*Figure 4*, yellow box).

For all the stems/primary branches, secondary branches, and tertiary branches in the LSA, there was a significant difference in SNR values between different TOF-MRA images (5.0T *vs.* 3.0T: P<0.05, *Figure 5A-5C*). Similarly, significant differences were also observed in CNR values (5.0T *vs.* 3.0T: P<0.05, *Figure 5D-5F*). *Table 4* shows the detailed LSA stems/branches quantitative measurement results and their comparison between 5.0T and 3.0T TOF-MRA. We found that regardless of the LSA stems and branches of different levels, 5.0T TOF-MRA was significantly better than 3.0T TOF-MRA, both in the display of vessel number and length. LSA tertiary branches were barely visible on the 3.0T TOF-MRA images, which made its quantitative measurements impossible. Overall, the radius of the branches at different levels measured at 3.0T and 5.0T are generally consistent: the radius measured at 5.0T is larger than that at 3.0T, but the difference is not significant.

5.0T TOF-MRA resolution optimization

As shown in *Figure 6* and *Table 2*, different resolution settings (0.3, 0.4, and 0.5 mm) in 5.0T TOF-MRA had a significant impact on the imaging quality (SNR and CNR) of all LSA branches (ANOVA, P<0.05 for all subplots in *Figure 6*). Specifically, (I) the imaging quality (SNR and CNR) with 0.5 and 0.4 mm resolution was significantly better (P<0.05) than that with 0.3 mm resolution for most LSA branches. However, the difference in imaging quality between 0.3 and 0.4 mm resolution for the SNR and CNR of secondary branches (*Figure 6B*,*6E*) and between 0.3 and 0.5 mm resolution for the CNR of tertiary branches (*Figure 6F*) was not significant (P>0.05). (II) The imaging quality (SNR and CNR) of the 0.4 and 0.5 mm resolution settings was comparable for most LSA branches (P>0.05), with the exception that the SNR of the trunk was significantly better at 0.5 mm resolution compared to 0.4 mm.

Further analysis of the differences in the detailed visualization of LSA branches between 0.4 and 0.5 mm resolution, as shown in *Table 5*, revealed that the length of LSA branches at all levels was significantly greater with the 0.4 mm resolution than with the 0.5 mm resolution (P<0.05). Compared to the 0.5 mm resolution, 5.0T TOF-MRA with 0.4 mm resolution showed a similar number of LSA stems and proximal branches, but more distal branches. Additionally, the radius of LSA branches at all levels appeared slightly larger with the 0.4 mm resolution, although this difference was not statistically significant (P>0.05).

Clinical application: follow-up and evaluation of the patient with left cerebral infarction

Figure 7 displays the visualization from three follow-up sessions of the patient with cerebral infarction, analyzed using our LSA hierarchical method based on 5.0T TOF-MRA, whereas *Table 6* presents the corresponding extracted LSA hierarchical parameters. As seen from the figure and table, the LSA branches on the affected side (left side) of the patient were the most abundant on one day after the onset of the disease. With the stability and recovery of the disease, all the total number, total length, and average radius of LSA branches gradually decreased (73 days after the symptom onset) and became stable (126 days after the symptom onset). Additionally, it is notable that in each follow-up, the patient exhibited a significantly higher number of LSA on the left side compared to the right. This may be due to vascular compensation after left cerebral infarction, or the lateralization of LSA itself, which needs

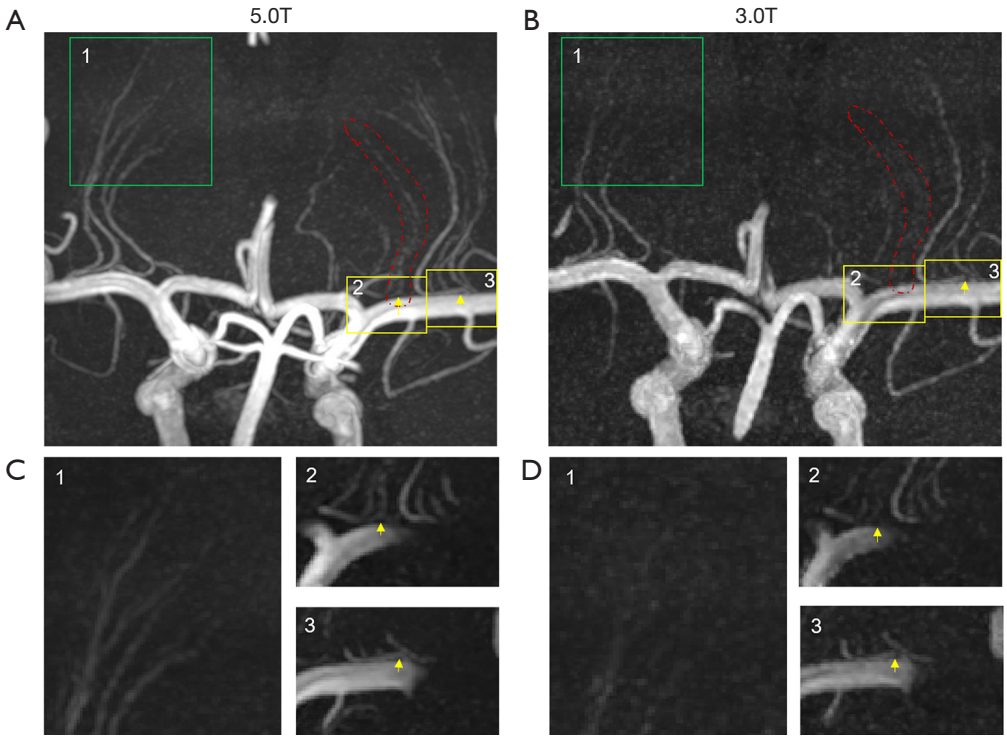

Figure 4 The maximum intensity projection images (A,B: slab thickness =20 mm; C,D: slab thickness =5 mm) of another volunteer (23-year-old female) on the 5.0T and 3.0T TOF-MRA. (A,B) Green rectangle box, the distal area of LSA; yellow rectangular box, the origin of LSA; red dashed box, some primary branches are visible with 5.0T TOF-MRA but not 3.0T TOF-MRA. (C,D) 1, the enlarged image of the green box; 2 and 3, the enlarged image of yellow rectangular box. LSA, lenticulostriate artery; TOF-MRA, time-of-flight magnetic resonance angiography.

further evidence to verify.

Discussion

The TOF-MRA sequence is primarily used for imaging major intracranial arteries; however, imaging the LSA is challenging due to their small diameter and tortuous course. Currently, only a few LSA branches can be visualized using 1.5T MRI (9). Although 3.0T MRI can delineate the anatomical structure of the LSA, its resolution and SNR are limited, and only a few studies have described the complex multilevel branching of the LSA (7,8,15). In practice, we have observed that the visualization of different LSA segments varies with MRI field strength and sequence, and that clinicians focus on different LSA regions. Simply classifying the LSA into major and smaller branches does not accurately reflect the image quality at different field strengths, nor does it fully reveal the potential of advanced imaging technologies in enhancing LSA visualization and meeting clinical demands. In this study, we proposed a stratified quantitative evaluation method to assess the number and quality of each LSA segment using 5.0T TOF-MRA and 3.0T TOF-MRA. We also performed a comparative analysis of 5.0T TOF-MRA at three different resolutions to provide clearer guidance for its clinical application in LSA imaging. Our results showed that the number and length of different LSA branches visualized by 5.0T TOF-MRA exceed those seen with 3.0T, particularly in the proximal stem and distal tertiary branches. Therefore, when the focus shifts to imaging the initial or distal segments of the LSA, 5.0T MRI holds significant potential in both clinical and research settings.

In our quantitative comparison of 5.0T and 3.0T TOF-MRA, we observed a significant improvement with 5.0T in visualizing the proximal segment of the LSA from the MCA, as shown in *Figure 4C,4D*. During the process of tracing and quantifying the LSA, we found that identifying the proximal segment of the LSA on 3.0T TOF-MRA is particularly difficult. This difficulty is due to the fact that, unlike the schematic illustrations in textbooks that

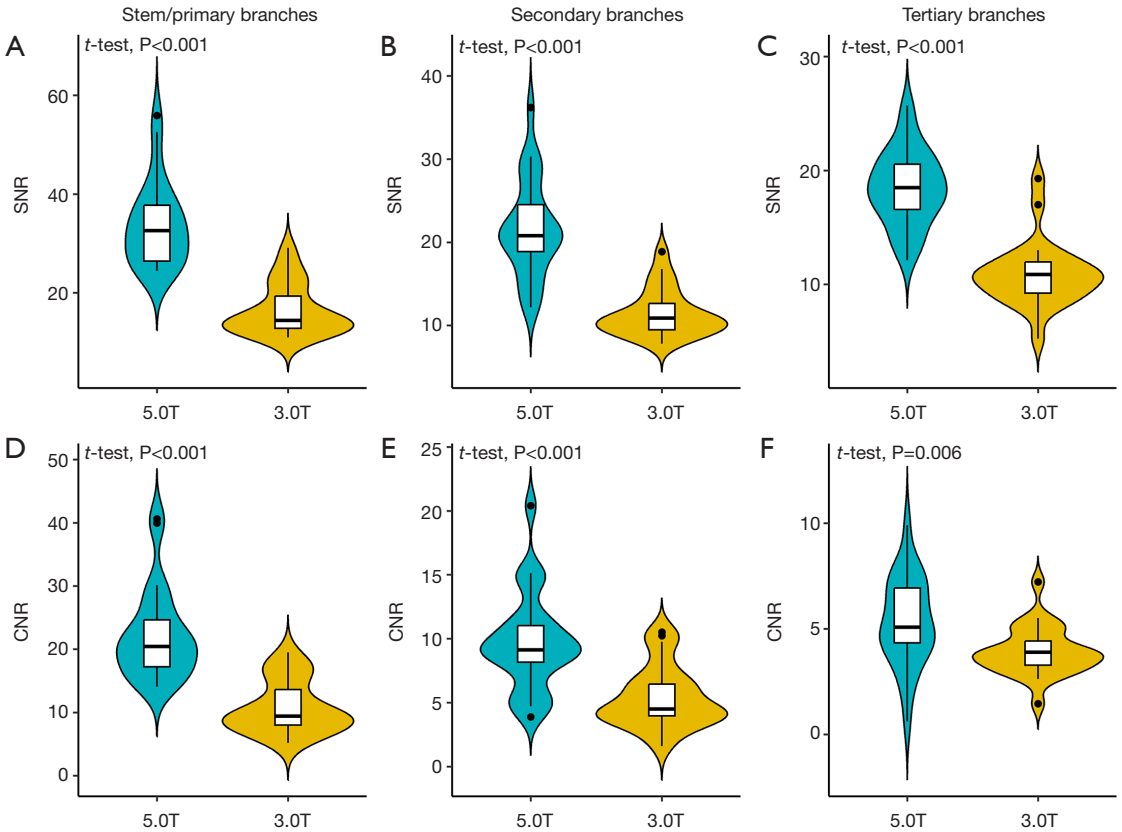

Figure 5 Comparison of LSA imaging quality between 5.0T and 3.0T TOF-MRA (based on SNR and CNR). (A-C) The first row of the figure shows the comparison result using SNR index, whereas (D-F) the second shows that using CNR index. From left to right, the comparison results for stem/primary, secondary, and tertiary branches are shown. Paired *t*-test was used in the comparison between 5.0T TOF-MRA and 3.0T TOF-MRA and the corresponding P values are shown in the left-top of each subplot. SNR, signal-to-noise ratio; CNR, contrast-to-noise ratio; LSA, lenticulostriate artery; TOF-MRA, time-of-flight magnetic resonance angiography.

Table 4 LSA hierarchic parameters measurement results (mean ± standard deviation) between 3.0T and 5.0T TOF-MRA

Parameters	3.0T TOF-MRA	5.0T TOF-MRA	*t*	P value
Stem Num.	4.73±1.62	6.36±2.11	−2.46	0.033*
Stem Radius (mm)	0.45±0.13	0.52±0.15	−2.17	0.053
Total Branch Num.	10.9±3.36	17.83±3.71	−5.51	<0.001***
Total Len. (mm)	217.84±50.69	387.56±66.06	−11.03	<0.001***
Primary Num.	6.91±1.64	9.36±1.43	−3.94	0.03*
Primary Len. (mm)	178.60±53.97	296.72±38.21	−10.10	<0.001***
Primary Radius (mm)	0.22±0.08	0.28±0.07	−2.58	0.260
Secondary Num. (mm)	4.00±2.32	7.09±2.98	−2.77	0.020*
Secondary Len.	39.24±19.86	80.58±39.87	−2.93	0.015*
Secondary Radius (mm)	0.14±0.03	0.16±0.03	−1.20	0.255
Tertiary Num.	0.00±0.00	1.36±1.12	−4.04	0.002**
Tertiary Len. (mm)	0.00±0.00	10.25±12.64	−2.69	0.023*

*, P<0.05; **, P<0.01; ***, P<0.001. LSA, lenticulostriate artery; TOF-MRA, time-of-flight magnetic resonance angiography; Num., number; Len., length.

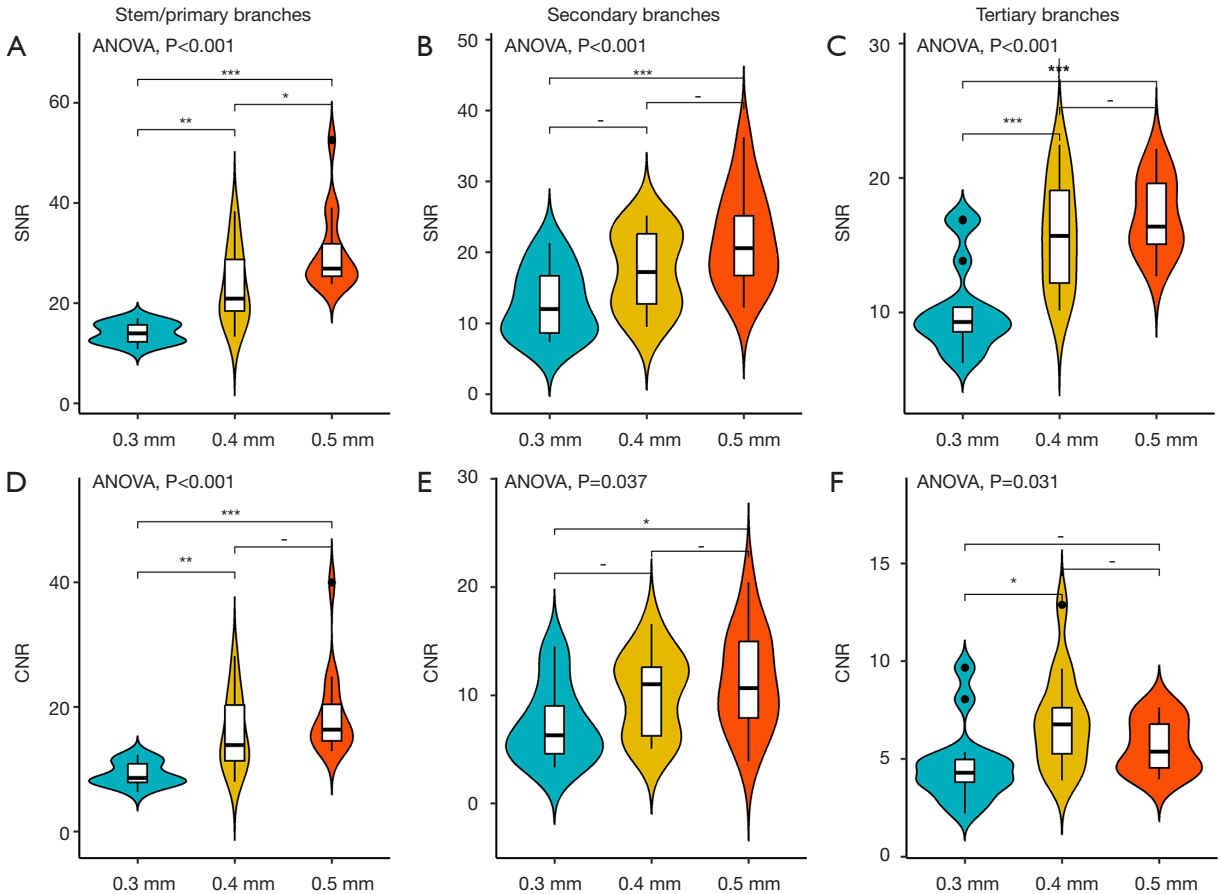

Figure 6 Comparison of LSA imaging quality using 5.0T TOF-MRA with different resolution setting (based on SNR and CNR). (A-C) The first row of the figure shows the comparison result using SNR index, whereas (D-F) the second shows that using CNR index. From left to right, the comparison results for stem/primary, secondary, and tertiary branches are shown. ANOVA is used to test whether different resolution values have significant effects on image quality, with the corresponding P values were shown in each subplot. Bonferroni correction was used for the multiple comparison between different resolutions pairs (0.3 *vs.* 0.4, 0.4 *vs.* 0.5 and 0.3 *vs.* 0.5 mm). Significance levels for these comparisons are indicated as follows: -, P>0.05, *, P<0.05; **, P<0.01; ***, P<0.001. ANOVA, analysis of variance; SNR, signal-to-noise ratio; CNR, contrast-to-noise ratio; LSA, lenticulostriate artery; TOF-MRA, time-of-flight magnetic resonance angiography.

depict the predominant orientation of LSA branches as perpendicular to the trajectory of the MCA, the majority of the perforators actually coursed medially, parallel to, or along the M1 segment toward the internal carotid artery bifurcation (21). This has introduced two challenges in tracing efforts: firstly, when the initiation of multiple stems runs parallel to the MCA, the proximity between the trunks and branches of the LSA can intermittently create the appearance of vascular intersections, fostering the illusion of vascular anastomosis, which poses significant challenges for differentiating and tracing the proximal segment of the LSA; secondly, the proximal segment of LSA, which runs parallel to the MCA, aligns with the imaging plane in a parallel manner rather than perpendicularly. As a result, this segment of the blood flow signal is susceptible to saturation, making it difficult to display effectively.

The diminished contrast between vessels and surrounding tissues, coupled with the proximity of vessels, can easily lead to deceptive artifacts during automated tracking. Our research highlighted significant benefits of 5.0T MRA over 3.0T in this regard, due to the enhanced contrast between vascular and tissue structures. This substantially diminishes the illusions arising from automated

Table 5 LSA hierarchic parameters measurement results (mean ± standard deviation) between different resolution in 5.0T TOF-MRA

Parameters	0.5 mm × 0.5 mm	0.4 mm × 0.4 mm	*t*	P value
Stem Num.	6.13±1.96	6.13±1.96	NA	NA
Stem Radius (mm)	0.47±0.14	0.49±0.16	−1.66	0.140
Total Branch Num.	17.63±3.96	20.25±3.77	−4.93	0.002**
Total Len. (mm)	398.36±77.33	444.78±79.44	−6.01	<0.001***
Primary Num.	9.13±2.03	9.13±2.10	0	1.000
Primary Len. (mm)	282.43±45.78	297.63±42.57	−2.53	0.039*
Primary Radius (mm)	0.31±0.16	0.32±0.07	−1.27	0.246
Secondary Num. (mm)	6.50±2.51	7.75±2.82	−3.04	0.019*
Secondary Len.	97.06±42.71	116.74±49.67	−5.42	<0.001***
Secondary Radius (mm)	0.15±0.03	0.16±0.04	−1.30	0.234
Tertiary Num.	2.00±1.51	3.38±1.60	−5.23	0.001**
Tertiary Len. (mm)	18.86±20.19	30.41±27.10	−3.49	0.010*

*, P<0.05; **, P<0.01; ***, P<0.001. LSA, lenticulostriate artery; TOF-MRA, time-of-flight magnetic resonance angiography; Num., number; Len., length.

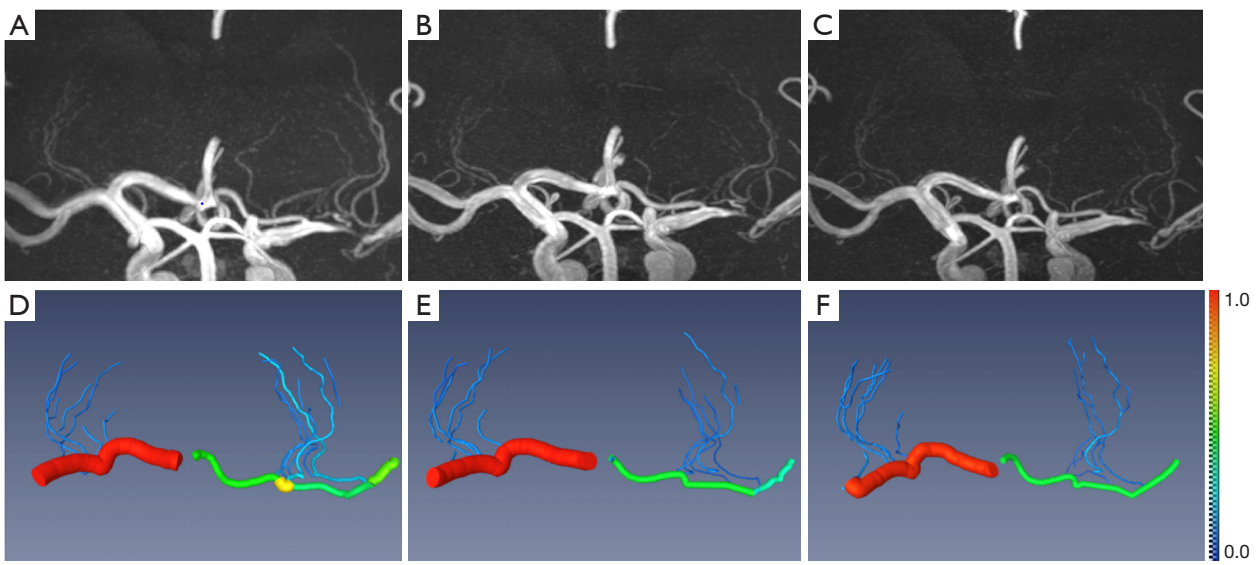

Figure 7 An example of the imaging result for a cerebral infarction patient during three follow-ups in four months. (A-F) Correspond to distinct views and analyses of the data at each follow-up time point. From left to right, the results of three follow-up visits for the patient were shown respectively, with a follow-up time points at 1 day (first), 73 days (second), and 126 days (third) after the symptom onset; from top to bottom were the 5.0T TOF-MRA images and tracked results for each follow-up. TOF-MRA, time-of-flight magnetic resonance angiography.

tracking and subsequent manual corrections. This advantage mainly arises from the heightened saturation of background tissues and reduced background signal in 5.0T compared to 3.0T, which enhances the relative signal of the proximal LSA. Some studies have indicated a significant concern of stenting in patients with intracranial stenosis is the risk of perforator stroke, which involves the occlusion of perforator arteries from the stent struts crossing the ostia of these arteries (22-24). Tracing the origin of the LSA and providing clarity can be advantageous for stent implantation

Table 6 The change of LSA hierarchic parameters during three follow-ups

Parameters	Left			Right		
	First	Second	Third	First	Second	Third
Stem Num.	3	3	3	4	4	4
Stem Radius (mm)	0.50	0.44	0.42	0.42	0.42	0.41
Total Branch Num.	11	9	8	9	8	7
Total Len. (mm)	227.10	180.30	168.90	138.71	133.95	102.38
Primary Num.	6	4	4	4	4	3
Primary Len. (mm)	173.21	139.81	135.43	84.99	88.67	66.70
Primary Radius (mm)	0.23	0.20	0.20	0.19	0.19	0.18
Secondary Num.	3	5	4	5	4	4
Secondary Len. (mm)	41.88	40.49	33.47	53.72	45.28	35.68
Secondary Radius (mm)	0.12	0.11	0.11	0.13	0.12	0.12
Tertiary Num.	2	0	0	0	0	0
Tertiary Len. (mm)	12.01	0.00	0.00	0.00	0.00	0.00

First: 1 day after the symptom onset. Second: 73 days after the symptom onset. Third: 126 days after the symptom onset. LSA, lenticulostriate artery; Num., number; Len., length.

in patients with MCA stenosis, potentially reducing the risk of perforation.

The quantitative analysis of 5.0T and 3.0T TOF-MRA showed that 5.0T TOF-MRA enhances the visualization of the distal and tiny branches of the LSA. Remarkably, 5.0T TOF-MRA is capable of clearly depicting numerous tertiary branches that are not discernible with 3.0T TOF-MRA. Additionally, there is a marked improvement in imaging the minute branches originating from the MCA. On 3.0T MRA, due to the reduced blood flow and smaller diameter of LSA tertiary branches (1,11), the inflow enhancement effect is diminished, resulting in near-invisibility. In contrast, 5.0T TOF-MRA significantly improves the visibility of tertiary and minute branches. In our study, 5.0T displayed 221 branches compared to the 133 branches displayed on 3.0T. This advancement can contribute to the construction of a more comprehensive vascular network of LSA, enabling the detection of subtle changes in tertiary branches of LSA in hypertensive or cerebral infarction patients, thus facilitating better control and therapeutic interventions for these conditions.

To optimize the imaging parameters of the 5.0T ultra-high magnetic field, we explored the impact of different resolutions on the quality of LSA imaging at 5.0T TOF-MRA. Our study revealed that considering both temporal efficiency and image quality, it is prudent to select a resolution of 0.4 mm (9 minutes 35 seconds) for 5.0T TOF-MRA, which is particularly effective for visualizing small distal branches. As detailed in *Table 5* and *Figure 6*, at a resolution of 0.4 mm, the lengths of LSA branches at all hierarchical levels depicted by 5.0T TOF-MRA exceeded those shown at 0.5 mm. Furthermore, the radius of the LSA branches at all levels, at a resolution of 0.4 mm, displayed a slightly larger magnitude compared to the 0.5 mm setting, although the observed difference did not reach statistical significance. When the resolution was further increased to 0.3 mm (12 minutes 18 seconds), a noticeable decline in image quality occurred due to the reduced SNR. Although an increase in SNR may theoretically result in better imaging outcomes, the constraint of time and patient comfort argue against this approach. Therefore, we recommend against the pursuit of higher resolution at the cost of imaging duration, as it represents an unwarranted trade-off.

A follow-up case study of the patient with putamen infarction was presented to illustrate the efficacy of 5.0T TOF-MRA and the proposed hierarchical quantitative assessment methodology. The results revealed that within the initial day following the infarction, there was an increase

in the total number and radius of LSA, as well as in the count and radius of the primary and tertiary branches on the affected side, reaching their peak. This augmentation gradually decreased during the second and fourth month of follow-up examinations. It is believed that this phenomenon may be due to an acute compensatory mechanism, which is initially strengthened and then diminishes during the recovery phase. Literature suggests that individuals with longer average lengths of LSA exhibit diminished susceptibility to early neurological deterioration (25), indicating a potentially positive prognosis for the patient in question. These findings are consistent with the patient's sequential follow-up assessments. The number of secondary branches peaked at the 2-month mark and then gradually decreased. This could be ascribed to the ischemic lesion's proximity to the second and third branches, leading to compensatory vascular proliferation near the infarcted region. Based on these observations, it can be concluded that the hierarchical quantitative assessment method, combined with 5.0T TOF-MRA, provides a powerful tool for the quantitative analysis of subtle changes in the LSA.

Limitations

There are a few limitations in our study. Firstly, the 3D tracking method adopted is semi-automatic, requiring manual intervention, especially when tracking small branches and in complex areas such as the proximal segment, which may be susceptible to the subjective biases of researchers. The development of advanced automatic segmentation and reconstruction techniques for LSA is crucial, promising a more streamlined image post-processing and an unbiased measure of LSA in future studies. Secondly, this investigation represents a pioneering venture in utilizing the branching pattern as a means to delineate the multi-tiered branches of LSA. The outcomes detailing LSA branching patterns lack a comparative analysis with alternative modalities such as computed tomography (CT) angiography. Finally, this is a preliminary study that included a relatively limited number of participants. The change of LSA, along with its neurophysiological implications warrants careful evaluation in larger populations and patients with cerebrovascular diseases in the future.

Conclusions

Our findings suggest that 5.0T TOF-MRA employing the hierarchic analysis method emerges as a promising imaging modality for the comprehensive assessment of LSA. This method has the potential to accelerate the investigation into the etiological factors and the development of personalized interventions for conditions including stroke, cerebral small vessel disease, and intracranial atherosclerosis.

Acknowledgments

None.

Footnote

Funding: None.

Conflicts of Interest: All authors have completed the ICMJE uniform disclosure form (available at https://qims.amegroups.com/article/view/10.21037/qims-24-1554/coif). X.S. is an employee of MR Collaboration, Central Research Institute, United Imaging Healthcare; and Wuhan Zhongke Industrial Research Institute of Medical Science. The other authors have no conflicts of interest to declare.

Ethical Statement: The authors are accountable for all aspects of the work in ensuring that questions related to the accuracy or integrity of any part of the work are appropriately investigated and resolved. The study was conducted in accordance with the Declaration of Helsinki (as revised in 2013). The study was approved by the Medical Ethics Committee of Zhongnan Hospital of Wuhan University (No. 2021110), and all participants provided written informed consent.

References

1. Marinkovic S, Gibo H, Milisavljevic M, Cetkovic M. Anatomic and clinical correlations of the lenticulostriate arteries. Clin Anat 2001;14:190-5.

2. Donzelli R, Marinkovic S, Brigante L, de Divitiis O, Nikodijevic I, Schonauer C, Maiuri F. Territories of the perforating (lenticulostriate) branches of the middle cerebral artery. Surg Radiol Anat 1998;20:393-8.
3. Chen YC, Wei XE, Lu J, Qiao RH, Shen XF, Li YH. Correlation Between the Number of Lenticulostriate Arteries and Imaging of Cerebral Small Vessel Disease. Front Neurol 2019;10:882.
4. Willinek WA, Born M, Simon B, Tschampa HJ, Krautmacher C, Gieseke J, Urbach H, Textor HJ, Schild HH. Time-of-flight MR angiography: comparison of 3.0-T imaging and 1.5-T imaging--initial experience. Radiology 2003;229:913-20.
5. Fushimi Y, Miki Y, Kikuta K, Okada T, Kanagaki M, Yamamoto A, Nozaki K, Hashimoto N, Hanakawa T, Fukuyama H, Togashi K. Comparison of 3.0- and 1.5-T three-dimensional time-of-flight MR angiography in moyamoya disease: preliminary experience. Radiology 2006;239:232-7.
6. Okuchi S, Okada T, Fujimoto K, Fushimi Y, Kido A, Yamamoto A, Kanagaki M, Dodo T, Mehemed TM, Miyazaki M, Zhou X, Togashi K. Visualization of Lenticulostriate Arteries at 3T: Optimization of Slice-selective Off-resonance Sinc Pulse–prepared TOF-MRA and Its Comparison with Flow-sensitive Black-blood MRA. Academic Radiology 2014;21:812-6.
7. Akashi T, Taoka T, Ochi T, Miyasaka T, Wada T, Sakamoto M, Takewa M, Kichikawa K. Branching pattern of lenticulostriate arteries observed by MR angiography at 3.0 T. Jpn J Radiol 2012;30:331-5.
8. Chen YC, Li MH, Li YH, Qiao RH. Analysis of correlation between the number of lenticulostriate arteries and hypertension based on high-resolution MR angiography findings. AJNR Am J Neuroradiol 2011;32:1899-903.
9. Gotoh K, Okada T, Miki Y, Ikedo M, Ninomiya A, Kamae T, Togashi K. Visualization of the lenticulostriate artery with flow-sensitive black-blood acquisition in comparison with time-of-flight MR angiography. J Magn Reson Imaging 2009;29:65-9.
10. Kang CK, Park CW, Han JY, Kim SH, Park CA, Kim KN, Hong SM, Kim YB, Lee KH, Cho ZH. Imaging and analysis of lenticulostriate arteries using 7.0-Tesla magnetic resonance angiography. Magn Reson Med 2009;61:136-44.
11. Bouvy WH, Biessels GJ, Kuijf HJ, Kappelle LJ, Luijten PR, Zwanenburg JJ. Visualization of perivascular spaces and perforating arteries with 7 T magnetic resonance imaging. Invest Radiol 2014;49:307-13.
12. Ma SJ, Sarabi MS, Yan L, Shao X, Chen Y, Yang Q, Jann K, Toga AW, Shi Y, Wang DJJ. Characterization of lenticulostriate arteries with high resolution black-blood T1-weighted turbo spin echo with variable flip angles at 3 and 7 Tesla. Neuroimage 2019;199:184-93.
13. Cho ZH, Kang CK, Han JY, Kim SH, Kim KN, Hong SM, Park CW, Kim YB. Observation of the lenticulostriate arteries in the human brain in vivo using 7.0T MR angiography. Stroke 2008;39:1604-6.
14. Kang CK, Park CA, Park CW, Lee YB, Cho ZH, Kim YB. Lenticulostriate arteries in chronic stroke patients visualised by 7 T magnetic resonance angiography. Int J Stroke 2010;5:374-80.
15. Kang CK, Park CA, Lee H, Kim SH, Park CW, Kim YB, Cho ZH. Hypertension correlates with lenticulostriate arteries visualized by 7T magnetic resonance angiography. Hypertension 2009;54:1050-6.
16. Hendrikse J, Zwanenburg JJ, Visser F, Takahara T, Luijten P. Noninvasive depiction of the lenticulostriate arteries with time-of-flight MR angiography at 7.0 T. Cerebrovasc Dis 2008;26:624-9.
17. Shi Z, Zhao X, Zhu S, Miao X, Zhang Y, Han S, Wang B, Zhang B, Ye X, Dai Y, Chen C, Rao S, Lin J, Zeng M, Wang H. Time-of-Flight Intracranial MRA at 3 T versus 5 T versus 7 T: Visualization of Distal Small Cerebral Arteries. Radiology 2023;306:207-17.
18. Wei Z, Chen Q, Han S, Zhang S, Zhang N, Zhang L, Wang H, He Q, Cao P, Zhang X, Liang D, Liu X, Li Y, Zheng H. 5T magnetic resonance imaging: radio frequency hardware and initial brain imaging. Quant Imaging Med Surg 2023;13:3222-40.
19. Chen H, Tang R, Song X, Zong R, Liu J, Jin C, Deng K. Comparison of single shot and multishot diffusion-weighted imaging in 5-T magnetic resonance imaging for brain disease diagnosis. Quant Imaging Med Surg 2024;14:7291-305.
20. Wardlaw JM, Dennis MS, Warlow CP, Sandercock PA. Imaging appearance of the symptomatic perforating artery in patients with lacunar infarction: occlusion or other vascular pathology? Ann Neurol 2001;50:208-15.
21. Djulejić V, Marinković S, Milić V, Georgievski B, Rašić M, Aksić M, Puškaš L. Common features of the cerebral perforating arteries and their clinical significance. Acta Neurochir (Wien) 2015;157:743-54; discussion 754.
22. Levy EI, Chaturvedi S. Perforator stroke following

intracranial stenting: a sacrifice for the greater good? Neurology 2006;66:1803-4.
23. Jiang WJ, Srivastava T, Gao F, Du B, Dong KH, Xu XT. Perforator stroke after elective stenting of symptomatic intracranial stenosis. Neurology 2006;66:1868-72.
24. Sasaki T, Kodama N, Matsumoto M, Suzuki K, Konno Y, Sakuma J, Endo Y, Oinuma M. Blood flow disturbance in perforating arteries attributable to aneurysm surgery. J Neurosurg 2007;107:60-7.
25. Yan Y, Jiang S, Yang T, Yuan Y, Wang C, Deng Q, Wu T, Tang L, Wu S, Sun J, Wu B. Lenticulostriate artery length and middle cerebral artery plaque as predictors of early neurological deterioration in single subcortical infarction. Int J Stroke 2023;18:95-101.

Cite this article as: Mei H, Lv J, Xu D, Gao L, Sun W, Zhong X, Fan C, Tao R, Song X, Xiao F, Xu H. 3D time-of-flight magnetic resonance angiography of lenticulostriate artery imaging at 5.0 Tesla: a hierarchic analysis method and clinical applications. Quant Imaging Med Surg 2025;15(3):1768-1783. doi: 10.21037/qims-24-1554

